When Anthracene and Quinone Avoid Cycloaddition: Acid-Catalyzed Redox Neutral Functionalization of Anthracene to Aryl Ethers
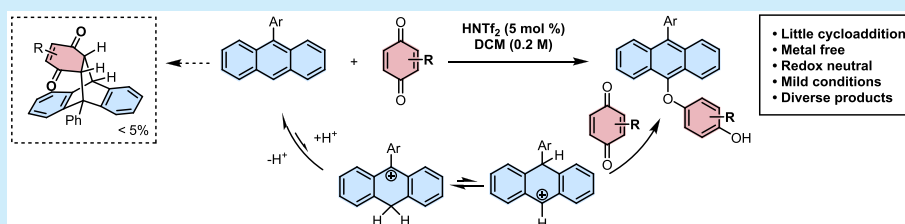
Nan Ding and Zhi Li*

ACCESS | Metrics & More | Article Recommendations | SI Supporting Information

ABSTRACT: Benzoquinone and 9-phenylanthracene barely undergo anticipated cycloaddition under acid catalysis. Instead, 9-anthracenyl aryl ethers are obtained as unexpected products. Mechanistic studies indicate that the reaction likely undergoes an ionic mechanism between protonated anthracene species and nucleophilic oxygen of 1,4-benzoquinone or 1,4-hydroquinone. A variety of 9-anthracenyl aryl ethers are constructed with this method. Produced anthracenyl aryl ethers are potential scaffolds for new fluorescent molecules.

Anthracene and derivatives are molecules of elegant structures and versatile functions. Anthracene-derived chromophores enabled many stable fluorescent organic light-emitting diode materials.[1] Its rigid structure has also been incorporated in the assembly of many metal−organic framework and covalent organic framework materials as a supporting unit.[2] In asymmetric catalysis, substituted anthracenyl groups are popular elements for introducing unique steric and electronic effects into chiral catalysts.[3] Moreover, the 1,8-sites and 9,10-sites were frequently functionalized to construct multidentate ligands for metal complexes.[4] Strategies to access substituted anthracenes include metal-catalyzed cross-coupling reactions of prefunctionalized anthracenyl precursors,[5] alkylation through C−H deprotonation with strong base,[6] acid-promoted reactions such as Friedel−Crafts alkylation, acylation and other electrophilic substitution reactions,[7] as well as reactions of anthracenyl radical cations (Scheme 1a).[8]

One unique reaction pattern of anthracene as well as other linear polyaromatic hydrocarbons is participation in pericyclic reactions as a diene (Scheme 1b).[9] Anthracene is capable of both thermal and photochemical [4 + 2] or [4 + 4] cycloadditions with various dienophiles or dienes across the 9,10-sites.[9a,10] Meanwhile, quinones are very common dienophiles that can certainly react with anthracene in Diels−Alder reactions, especially so when catalyzed by Lewis acids.[10b,11] However, we observed that, under a strong Brønsted acid catalysis environment using bis(trifluoromethanesulfon)imide (Tf$_2$NH) as the catalyst, Diels−Alder reaction between 9-phenylanthracene (PA, **1a**) and 1,4-

benzoquinone (Q, **2a**) only contributes a very minor fraction of the product mixture (<5%). Instead, the major product is identified by single crystal X-ray diffraction as 4-((10-phenylanthracen-9-yl)oxy)phenol (PAOP, **3aa**), in which a new C−O bond was formed connecting the 10-position of PA and one hydroxyl of a 1,4-hydroquinone (HQ) fragment (Scheme 1c). Here we report the preliminary mechanistic investigation of this unexpected transformation as well as its applications in the synthesis of anthracenyl aryl ethers.

Reaction condition studies revealed that the acidity of catalysts is likely a vital factor in this catalytic reaction. PA and Q were treated with a series of Lewis acids and Brønsted acids as the catalyst, giving PAOP as the major product. HNTf$_2$ is the best catalyst among those examined (Table 1, entries 1−6).[12] Without the acid catalyst, the reaction did not occur (Table 1, entry 2). Polar solvents or lower temperature reduced the yield (Table 1, entries 7−9). Q cannot be replaced by HQ under standard catalytic conditions (Table 1, entry 11). Thus, conditions of Table 1, entry 1 are adapted as the standard conditions (see Table S1 in the Supporting Information for a full list of conditions). A 1 mmol scale
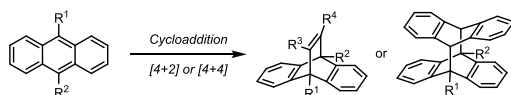
Scheme 1. Synthetic Strategies and Reactions of Anthracene Derivatives

(a) Classic methods of anthracene functionalization
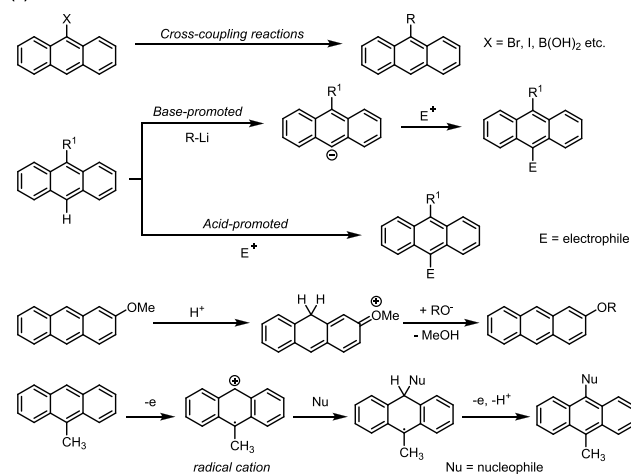
(b) Pericyclic reactions of anthracene

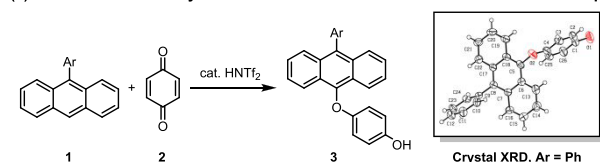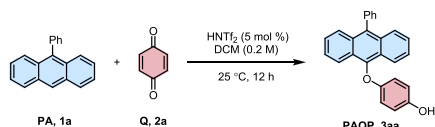(c) This work: acid-catalyzed C−O bond construction between anthracene and quinone

Crystal XRD, Ar = Ph

Table 1. Conditions Optimization of PAOP Formation

entry	variation from standard conditions[a]	yield/%[b]
1	no variation	85 (75)
2	no HNTf$_2$	NR
3	catalyst = 5 mol % Cu(NTf$_2$)$_2$	30
4	catalyst = 5 mol % Sc(NTf$_2$)$_3$	47
5	catalyst = 5 mol % Hf(OTf)$_4$	56
6	catalyst = 5 mol % TfOH	65
7	solvent = DCE	70
8	solvent = PhCF$_3$	57
9	solvent = dioxane	NR
10	temperature = 0 °C	61
11	HQ instead of Q	NR

[a]Standard conditions: **1a** (0.2 mmol), **2a** (0.2 mmol), 5 mol % HNTf$_2$ and DCM (1 mL) stirred at 25 °C for 12 h unless otherwise noted. Tf, trifluoromethanesulfonyl; DCM, dichloromethane; DCE, 1,2-dichloroethane; NR, no desired product. [b]Yields determined by crude ^{1}H NMR versus an internal standard C$_2$H$_2$Cl$_4$. Isolated yield in parentheses.

Scheme 2. Proposed Mechanism of PAOP Formation

catalysis commences with protonation of PA to PA−H$^+$ and its tautomer PA−H^{+*},[13] which could then be attacked by the adventitious HQ with one of its OH groups, forming the C−O bond after a final deprotonation. The resulting dihydroanthracene derivative (PAOP−H$_2$) contains two benzylic C−H bonds; thus, it is susceptible to oxidative aromatization toward PAOP.[14] It would be oxidized by the remaining Q to PAOP along with replenished HQ ready for the next cycle of reaction, propagating the redox chain.[15] In an alternatively proposed pathway B, PA−H$^+$ may react directly with Q, generating a redox active oxonium ion PAH$_2$−Q$^+$ as the key intermediate (Scheme 2b). This intermediate may function as an oxidant using the activated benzoquinone motif and as a reductant using the 9,10-dihydroanthracene motif. Thus, PAOP could be generated from this intermediate via an autoredox reaction. Here, the autoredox reaction probably traverses the same intermediate PAOP−H$_2$ as in pathway A, which could act as the initiator to start the redox chain. The point of divergence distinguishing pathways A and B is whether the carbocation intermediate PA−H$^+$ reacts with a −OH group of HQ or an oxygen of Q. We also considered the possibility of a radical cation mechanism initiated by protonation of Q and subsequent oxidation of PA to radical cation PA$^{•+}$,[16] but experimental evidence showed otherwise, which is described below.

Mechanism probing experiments were performed to test these hypotheses as well as a few others, and evidence suggests that the real mechanism may involve both ionic hypotheses working concurrently. First, protonation of anthracene is decisively proved by 10-deuteration of PA catalyzed by HNTf$_2$ (Scheme 3a). In fact, when Q was added to the deuteration condition, a similar level of PA-10-d can be recovered (25% D) along with PAOP-d, indicating the protonation reaction is parallelly operating with the PAOP formation (Scheme 3b). Second, when 4-methoxyphenol was added along with Q, the reaction generated not only 20% PAOP but also 55% PAOP-

reaction gave 73% isolated yield (see Supporting Information section III-(4)).

The structure of this unusual aryl ether left us hints to suggest a few preliminary mechanistic models for its formation. First, a redox chain mechanism based on quinone chemistry is proposed as pathway A (Scheme 2a). In this scenario, the
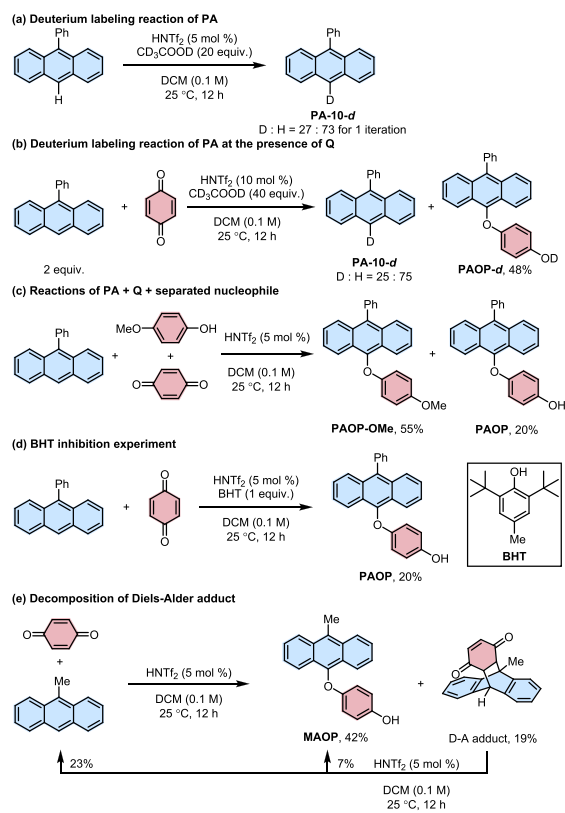
Scheme 3. Mechanism Probing Experiments

OMe, the C−O bond formation product between PA and 4-methoxyphenol. It appears that 4-methoxyphenol participated in the reaction as a surrogate of HQ through pathway A (Scheme 3c). However, generation of PAOP could not be significantly accelerated by adding extra HQ (Table S1). There must be an even more rapid PAOP formation pathway that involves only PA, Q, and acid catalyst, such as pathway B.

On the other hand, the radical cation pathway can be ruled out by the following facts. First, addition of 1 equiv of radical scavenger 2,6-di-tert-butyl-4-methylphenol (BHT) slowed down the reaction instead of complete inhibition, suggesting other nonradical pathways are present (Scheme 3d). Second, aliquots of the reaction between PA + Q were regularly monitored by electron paramagnetic resonance (EPR), but no single electron species was observed (Figure S1). Third, since the acid catalyst is essential, the hypothetical radical cation mechanism must begin with protonation of Q in order to level up its oxidation potential to oxidize PA to corresponding radical cation.[16b,17] However, cyclic voltammetry experiments showed that the oxidation potential of protonated Q is lower than that of PA and thus is unlikely to perform the oxidation (0.395 vs 0.763 V, Figure S2 of the Supporting Information). In addition, PA deuteration rates were about the same with or without Q, likely ruling out the possibility that a substantial amount of Q competes with PA for acidic protons.

Another mechanism possibility to be ruled out is decomposition of a potential intermediary Diels−Alder (D−A) adduct of a substituted anthracene and a quinone. The only D−A adduct stable enough to be isolated is that of 9-methylanthracene and Q, obtained in the same reaction to synthesize corresponding aryl anthracenyl ether 3va (Scheme

Scheme 4. Scope of Substituted Anthracenes and Benzoquinones[a]
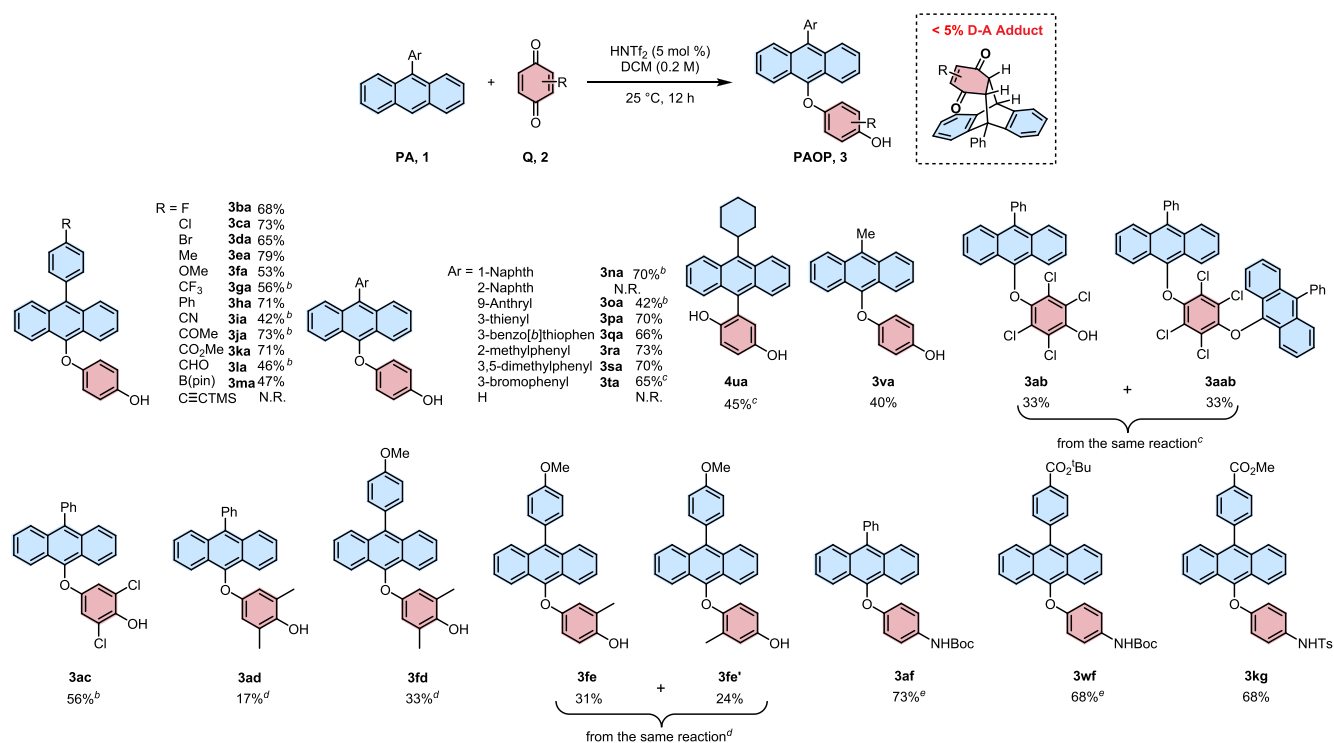
[a]Conditions: 1 (0.2 mmol), 2 (0.2 mmol), HNTf₂ (5 mol %), and DCM (1 mL) were stirred at 25 °C for 12 h unless otherwise noted. All yields are isolated yields after column chromatography. [b]1.5 equiv of 2, 30 °C, 24 h. [c]40 °C, 24 h. [d]20 mol % HNTf₂, 40 °C, 48 h. [e]2 equiv of p-benzoquinonimine 2f.

4). Upon treatment in the identical acid catalysis conditions, the adduct gave only 7% desired anthracenyl aryl ether product, along with 23% recovered 9-methylanthracene (Scheme 3e). These results suggest that the ether product likely emerges from the reaction between anthracene and Q resulting from the retro-Diels−Alder reaction following the above-mentioned mechanisms, rather than from the D−A adduct following acid-catalyzed fragmentation mechanism.

Kinetic studies were also performed. The Hammett relationship ($\rho = -6.61$ when varying the anthracene 9-substituents; see Figure S3 of the Supporting Information) indicated that a full carbocation is likely generated during the rate-determining step. The kinetic isotope effect (KIE) result ($k_H/k_D = 2.03$; see Figure S4 of the Supporting Information) indicated that the reaction does not involve direct C−H bond cleavage. The kinetic order of the catalyst (1.3 order for HNTf$_2$; see Figure S6 of the Supporting Information) suggests that the Brønsted acid might be involved in the rate-determining step in different forms, likely contributing to both pathways A and B that consume PA−H$^+$ in different rate laws. In summary of the mechanism, although the real mechanism is still perplexing, the ionic mechanisms initiated by protonation of PA are consistent with current evidence in hand.

Summarized in Scheme 4 are the substrate scopes of this reaction with respect to aryl anthracene derivatives/analogues and benzoquinones. Many functional groups on the anthracene were tolerated, including halogens, nitrile, aldehyde, ketone, ester, borate, and heterocycles (Scheme 4, 3ba−3ta). Cyclo-addition products were negligible in most cases, except for 9-methylanthracene which gave 10% of the cycloaddition byproduct along with 40% aryl ether (Scheme 4, 3va). Electron-withdrawing 9-substituents gave lower yield even at higher temperatures. 9-Cyclohexylanthracene gave a C−C bond formation product (4ua) instead of the C−O bond formation product. The benzoquinones capable of this transformation include substituted ones: methyl substituted quinones (3ad−3fe), chloranil, and 2,6-dichloroquinone (3ab, 3ac), but naphthoquinones and anthraquinones did not give any conversion. Moreover, N-protected p-benzoquinonimine also participated in this reaction, giving exclusively the C−O bond formation products (3af, 3wf, 3kg).

In the reaction between PA and chloranil, a considerable yield of the 2:1 coupling byproduct was obtained (Scheme 4, 3aab). In addition, formation of PAOP-OMe shown in Scheme 3c demonstrated that a phenolic nucleophile can be incorporated in the aryl ether at the presence of an oxidant. Therefore, additional examples following this strategy are summarized in Scheme 5. Structures derived from 1,4- and 1,2-hydroquinone achieved good yields (6aa−6ad). While using resorcinol, phloroglucinol, and trimethoxybenzene as nucleophiles, C−C bond formation products prevailed instead of C−O bond formation, resulting in biaryl compounds (6ae−6aag). Electron-donating substituents with a 1,3-substitution pattern on a benzene ring may synergistically enhance the nucleophilicity of the 2-, 4- and 6-positions, overriding the nucleophilicity of phenol hydroxyls. 2,3-Dihydroxynaphthalene also gave biaryl coupling product 6af. Even unsubstituted anthracene can be functionalized by trimethoxybenzene, giving 6xh as the product. N-Tosyl-protected p-aminophenol gave excellent yield of ether 6ai. Formation of all these products can be explained by mechanism pathway A. Note that when phenolic nucleophiles were used, coupling products between PA and

## Scheme 5. Scope of Nucleophiles in Reactions of PA with Separated Oxidants and Nucleophiles[a]
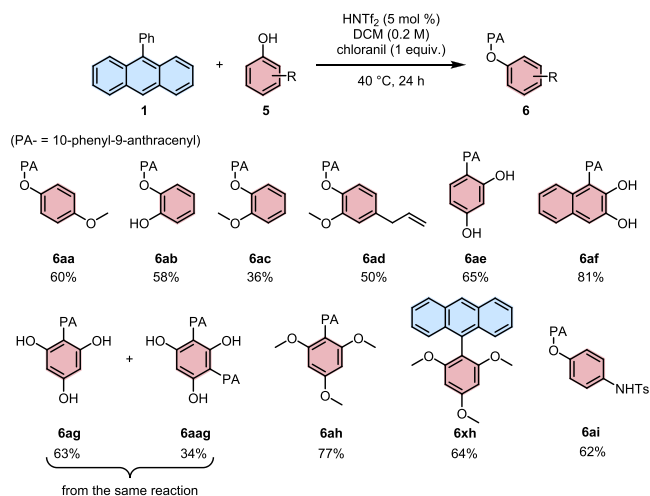
[a]Conditions: 1 (0.2 mmol), nucleophile 5 (0.2 mmol), chloranil (0.2 mmol), HNTf$_2$ (5 mol %), DCM (1 mL), 40 °C, 24 h. All yields are isolated yields after column chromatography.

chloranil (3ab, 3aab) were not observed, likely due to the lower nucleophilicity of tetrachlorohydroquinone/chloranil than that of electron-rich phenols.

Diversified PA-type substrates can be conveniently synthesized from easily accessible diarylmethyl carbinols or their acetates 7 under similar acid-catalyzed conditions.[18] Thus, a cascade reaction was developed, by simply adding Q and acid catalyst to the acetates, to achieve various PAOP-type aryl ethers that contain tunable polyaromatic motifs, aryl substituents, and phenolic motifs (Scheme 6, 3aa−8da).

## Scheme 6. Sequential Syntheses of Polycyclic Aryl Ethers[a]
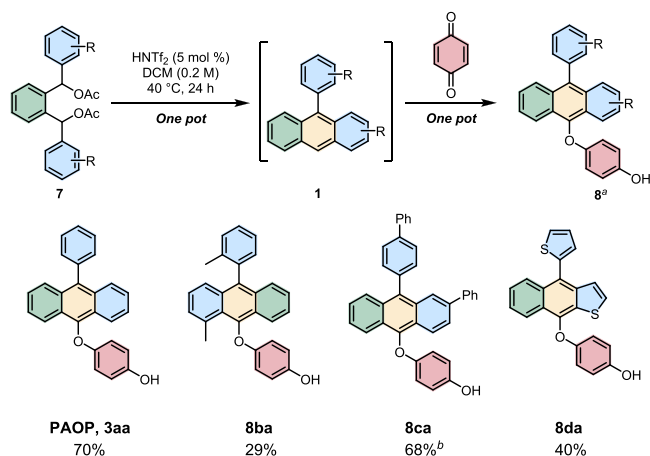
[a]Conditions: 7 (0.2 mmol), 2a (0.2 mmol), HNTf$_2$ (5 mol %), DCM (1 mL), 40 °C, 24 h. All yields are isolated yields after column chromatography. [b]1.5 equiv of 2a, 30 °C, 12 h.

All the anthracenyl-containing products synthesized in this study exhibit excellent fluorescence properties. Their utility in fluorescent labeling and detection can be preliminarily demonstrated by the convenient synthesis of an artificial fluorescent amino acid and its dopamine conjugate. A fluorescent dopamine analogue 11 exhibiting ex/em = 397/432 nm and fluorescent quantum yield (Φ_f) = 21.50% (Figure

S7) was made in four room temperature steps (Scheme 7). The emission wavelength of **11** does not overlap with the

Scheme 7. Anthracenyl Aryl Ether Derivatives as Fluorophore-Conjugated Dopamine in Bioimaging[a]
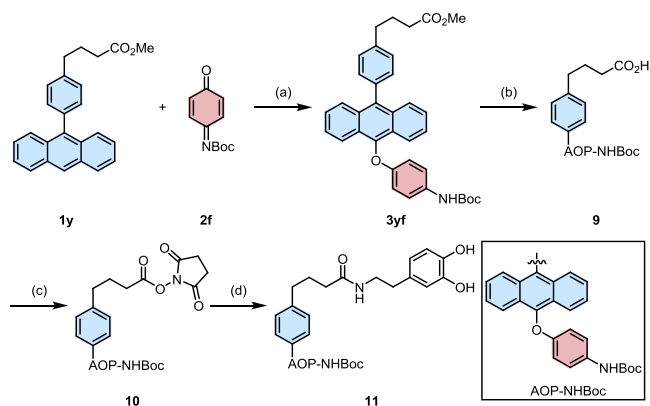
[a]Conditions: (a) HNTf$_2$ (5 mol %), DCM (0.2 M), rt, 12 h, 79%; (b) LiOH (6 equiv), MeOH/THF/H$_2$O = 1:1:1 (0.1 M), rt, 12 h, 90%; (c) N-hydroxysuccinimide (1.1 equiv), DCC (1.1 equiv), DCM (0.1 M), rt, 12 h, 90%; (d) dopamine hydrochloride (1.1 equiv), Et$_3$N (2.0 equiv), THF (0.1 M), rt, 12 h, 80%.

characteristic 495−529 nm fluorescence of Green Fluorescent Protein (GFP),[19] allowing orthogonal imaging of both dopamine-interacting domains and GFP-labeled domains simultaneously. Moreover, functional groups at **11** may allow further conjugation of a variety of targets with this fluorescent molecule. Imaging of biological systems with these fluorescence probes is underway.

In summary, we discovered a one-step, acid-catalyzed, metal-free, and redox neutral method to synthesize a series of anthracenyl aryl ethers that are difficult to access from other methods. Mechanistic experiments revealed possible ionic reaction sequences involving protonated anthracenes, phenolic nucleophiles, and benzoquinone oxidants. Applications of these new compounds are preliminarily investigated.

■ ASSOCIATED CONTENT

Supporting Information

The Supporting Information is available free of charge at https://pubs.acs.org/doi/10.1021/acs.orglett.0c01315.

> Details for optimization of the reactions, details for kinetic data, details for crystallographic data, details for electrical and optical properties of products, details for kinetic studies, experimental procedures, and characterization data (NMR, MS, X-ray) (PDF)

Accession Codes

CCDC 1970426 contains the supplementary crystallographic data for this paper. These data can be obtained free of charge via www.ccdc.cam.ac.uk/data_request/cif, or by emailing data_request@ccdc.cam.ac.uk, or by contacting The Cambridge Crystallographic Data Centre, 12 Union Road, Cambridge CB2 1EZ, UK; fax: +44 1223 336033.

■ AUTHOR INFORMATION

Corresponding Author

Zhi Li − School of Physical Science and Technology, ShanghaiTech University, Shanghai 201210, China; orcid.org/0000-0003-2770-6364; Email: lizhi@shanghaitech.edu.cn

Author

Nan Ding − School of Physical Science and Technology, ShanghaiTech University, Shanghai 201210, China; University of Chinese Academy of Sciences, Beijing 100049, China; Shanghai Institute of Organic Chemistry, Shanghai 200032, China

Complete contact information is available at:
https://pubs.acs.org/10.1021/acs.orglett.0c01315

Notes

The authors declare no competing financial interest.

■ REFERENCES

(1) (a) Moorthy, J. N.; Venkatakrishnan, P.; Natarajan, P.; Huang, D. F.; Chow, T. J. De Novo Design for Functional Amorphous Materials: Synthesis and Thermal and Light-Emitting Properties of Twisted Anthracene-Functionalized Bimesitylenes. J. Am. Chem. Soc. **2008**, 130 (51), 17320−17333. (b) Chen, M.; Zhao, Y.; Yan, L.; Yang, S.; Zhu, Y.; Murtaza, I.; He, G.; Meng, H.; Huang, W. A Unique Blend of 2-Fluorenyl-2-anthracene and 2-Anthryl-2-anthrance Showing White Emission and High Charge Mobility. Angew. Chem., Int. Ed. **2017**, 56 (3), 722−727. (c) Zhang, D.; Song, X.; Li, H.; Cai, M.; Bin, Z.; Huang, T.; Duan, L. High-Performance Fluorescent Organic Light-Emitting Diodes Utilizing an Asymmetric Anthracene Derivative as an Electron-Transporting Material. Adv. Mater. **2018**, 30 (26), 1707590.

(2) (a) Düren, T.; Sarkisov, L.; Yaghi, O. M.; Snurr, R. Q. Design of New Materials for Methane Storage. Langmuir **2004**, 20 (7), 2683−2689. (b) Ma, S. Q.; Sun, D. F.; Simmons, J. M.; Collier, C. D.; Yuan, D. Q.; Zhou, H. C. Metal-Organic Framework from an Anthracene Derivative Containing Nanoscopic Cages Exhibiting High Methane Uptake. J. Am. Chem. Soc. **2008**, 130 (3), 1012−1016. (c) Hauptvogel, I. M.; Biedermann, R.; Klein, N.; Senkovska, I.; Cadiau, A.; Wallacher, D.; Feyerherm, R.; Kaskel, S. Flexible and Hydrophobic Zn-Based Metal−Organic Framework. Inorg. Chem. **2011**, 50 (17), 8367−8374. (d) Chen, D. S.; Xing, H. Z.; Su, Z. M.; Wang, C. G. Electrical conductivity and electroluminescence of a new anthracene-based metal-organic framework with pi-conjugated zigzag chains. Chem. Commun. **2016**, 52 (10), 2019−2022. (e) Khayum, M. A.; Kandambeth, S.; Mitra, S.; Nair, S. B.; Das, A.; Nagane, S. S.; Mukherjee, R.; Banerjee, R. Chemically Delaminated Free-Standing Ultrathin Covalent Organic Nanosheets. Angew. Chem., Int. Ed. **2016**, 55 (50), 15604−15608. (f) Haldar, S.; Chakraborty, D.; Roy, B.; Banappanavar, G.; Rinku, K.; Mullangi, D.; Hazra, P.; Kabra, D.; Vaidhyanathan, R. Anthracene-Resorcinol Derived Covalent Organic Framework as Flexible White Light Emitter. J. Am. Chem. Soc. **2018**, 140 (41), 13367−13374.

(3) (a) Uraguchi, D.; Sorimachi, K.; Terada, M. Organocatalytic Asymmetric Direct Alkylation of α-Diazoester via C−H Bond Cleavage. J. Am. Chem. Soc. **2005**, 127 (26), 9360−9361. (b) Itoh,

J.; Fuchibe, K.; Akiyama, T. Chiral Brønsted Acid Catalyzed Enantioselective Aza-Diels−Alder Reaction of Brassard's Diene with Imines. *Angew. Chem., Int. Ed.* **2006**, *45* (29), 4796−4798. (c) Parmar, D.; Sugiono, E.; Raja, S.; Rueping, M. Complete Field Guide to Asymmetric BINOL-Phosphate Derived Brønsted Acid and Metal Catalysis: History and Classification by Mode of Activation; Brønsted Acidity, Hydrogen Bonding, Ion Pairing, and Metal Phosphates. *Chem. Rev.* **2014**, *114* (18), 9047−9153. (d) Feng, W.; Yang, H.; Wang, Z.; Gou, B. B.; Chen, J.; Zhou, L. Enantioselective [3 + 2] Formal Cycloaddition of 1-Styrylnaphthols with Quinones Catalyzed by a Chiral Phosphoric Acid. *Org. Lett.* **2018**, *20* (10), 2929−2933.

(4) (a) Haenel, M. W.; Oevers, S.; Angermund, K.; Kaska, W. C.; Fan, H. J.; Hall, M. B. Thermally Stable Homogeneous Catalysts for Alkane Dehydrogenation. *Angew. Chem., Int. Ed.* **2001**, *40* (19), 3596−3600. (b) Muckerman, J. T.; Polyansky, D. E.; Wada, T.; Tanaka, K.; Fujita, E. Water Oxidation by a Ruthenium Complex with Noninnocent Quinone Ligands: Possible Formation of an O−O Bond at a Low Oxidation State of the Metal. *Inorg. Chem.* **2008**, *47* (6), 1787−1802. (c) Boyer, J. L.; Rochford, J.; Tsai, M. K.; Muckerman, J. T.; Fujita, E. Ruthenium complexes with non-innocent ligands: Electron distribution and implications for catalysis. *Coord. Chem. Rev.* **2010**, *254* (3), 309−330. (d) Broere, D. L. J.; Plessius, R.; van der Vlugt, J. I. New avenues for ligand-mediated processes − expanding metal reactivity by the use of redox-active catechol, *o*-aminophenol and *o*-phenylenediamine ligands. *Chem. Soc. Rev.* **2015**, *44* (19), 6886−6915. (e) Low, C. H.; Rosenberg, J. N.; Lopez, M. A.; Agapie, T. Oxidative Coupling with Zr(IV) Supported by a Noninnocent Anthracene-Based Ligand: Application to the Catalytic Cotrimerization of Alkynes and Nitriles to Pyrimidines. *J. Am. Chem. Soc.* **2018**, *140* (38), 11906−11910. (f) Kerns, S. A.; Magtaan, A. C.; Vong, P. R.; Rose, M. J. Functional Hydride Transfer by a Thiolate-Containing Model of Mono-Iron Hydrogenase featuring an Anthracene Scaffold. *Angew. Chem., Int. Ed.* **2018**, *57* (11), 2855−2858.

(5) (a) Wan, C. W.; Burghart, A.; Chen, J.; Bergstrom, F.; Johansson, L. B. A.; Wolford, M. F.; Kim, T. G.; Topp, M. R.; Hochstrasser, R. M.; Burgess, K. Anthracene-BODIPY cassettes: Syntheses and energy transfer. *Chem. - Eur. J.* **2003**, *9* (18), 4430−4441. (b) Kotha, S.; Lahiri, K. Expanding the Diversity of Polycyclic Aromatics Through a Suzuki−Miyaura Cross-Coupling Strategy. *Eur. J. Org. Chem.* **2007**, *2007* (8), 1221−1236.

(6) López Ortiz, F.; Iglesias, M. J.; Fernández, I.; Andújar Sánchez, C. M.; Ruiz Gómez, G. Nucleophilic Dearomatizing (DNAr) Reactions of Aromatic C,H-Systems. A Mature Paradigm in Organic Synthesis. *Chem. Rev.* **2007**, *107* (5), 1580−1691.

(7) (a) Laali, K. K.; Arrica, M. A.; Okazaki, T.; Harvey, R. G. Substituent Effects in Benz[*a*]anthracene Carbocations: A Stable Ion, Electrophilic Substitution (Nitration, Bromination), and DFT Study. *J. Org. Chem.* **2007**, *72* (18), 6768−6775. (b) Sharghi, H.; Jokar, M.; Doroodmand, M. M.; Khalifeh, R. Catalytic Friedel−Crafts Acylation and Benzoylation of Aromatic Compounds Using Activated Hematite as a Novel Heterogeneous Catalyst. *Adv. Synth. Catal.* **2010**, *352* (17), 3031−3044. (c) Somai Magar, K. B.; Jebakumar Immanuel Edison, T. N.; Lee, Y. R. Regioselective synthesis of 3-anthracenyloxindoles and 3-carbazolyloxindoles by indium(III)-catalyzed direct arylation and their fluorescent chemosensor properties. *Org. Biomol. Chem.* **2016**, *14* (30), 7313−7323.

(8) (a) Cavalieri, E.; Rogan, E. Role of radical cations in aromatic hydrocarbon carcinogenesis. *Environ. Health Perspect.* **1985**, *64*, 69−84. (b) Cavalieri, E. L.; Rogan, E. G. The approach to understanding aromatic hydrocarbon carcinogenesis. The central role of radical cations in metabolic activation. *Pharmacol. Ther.* **1992**, *55* (2), 183−199. (c) Cremonesi, P.; Stack, D. E.; Rogan, E. G.; Cavalieri, E. L. Radical Cations of Benzo[*a*]pyrene and 6-Substituted Derivatives: Synthesis and Reaction with Nucleophiles. *J. Org. Chem.* **1994**, *59* (25), 7683−7687. (d) Cavalieri, E. L.; Rogan, E. G. Central role of radical cations in metabolic activation of polycyclic aromatic hydrocarbons. *Xenobiotica* **1995**, *25* (7), 677−688. (e) Lehner, A. F.; Horn, J.; Flesher, J. W. Formation of radical cations in a model for the metabolism of aromatic hydrocarbons. *Biochem. Biophys. Res. Commun.* **2004**, *322* (3), 1018−1023.

(9) (a) Thapaliya, E. R.; Captain, B.; Raymo, F. M. Photoactivatable Anthracenes. *J. Org. Chem.* **2014**, *79* (9), 3973−3981. (b) Guan, L.; Holl, M. G.; Pitts, C. R.; Struble, M. D.; Siegler, M. A.; Lectka, T. Through-Space Activation Can Override Substituent Effects in Electrophilic Aromatic Substitution. *J. Am. Chem. Soc.* **2017**, *139* (42), 14913−14916.

(10) (a) Atherton, J. C. C.; Jones, S. Diels−Alder reactions of anthracene, 9-substituted anthracenes and 9,10-disubstituted anthracenes. *Tetrahedron* **2003**, *59* (46), 9039−9057. (b) Zhao, L.; Li, Z.; Wirth, T. Triptycene Derivatives: Synthesis and Applications. *Chem. Lett.* **2010**, *39* (7), 658−667. (c) Maturi, M. M.; Fukuhara, G.; Tanaka, K.; Kawanami, Y.; Mori, T.; Inoue, Y.; Bach, T. Enantioselective [4 + 4] photodimerization of anthracene-2,6-dicarboxylic acid mediated by a C-2-symmetric chiral template. *Chem. Commun.* **2016**, *52* (5), 1032−1035. (d) Liu, W.; Guo, L.; Fan, Y.; Huang, Z.; Cong, H. [4 + 4] Photodimerization of Anthracene Derivatives: Recent Synthetic Advances and Applications. *Youji Huaxue* **2017**, *37* (3), 543−554. (e) Zhang, Q. C.; Lv, J.; Li, S. J.; Luo, S. Z. Carbocation Lewis Acid Catalyzed Diels-Alder Reactions of Anthracene Derivatives. *Org. Lett.* **2018**, *20* (8), 2269−2272.

(11) (a) Fukuzumi, S.; Okamoto, T. Magnesium perchlorate-catalyzed Diels-Alder reactions of anthracenes with p-benzoquinone derivatives: catalysis on the electron transfer step. *J. Am. Chem. Soc.* **1993**, *115* (24), 11600−11601. (b) Fukuzumi, S.; Ohkubo, K.; Okamoto, T. Metal Ion-Catalyzed Diels−Alder and Hydride Transfer Reactions. Catalysis of Metal Ions in the Electron-Transfer Step. *J. Am. Chem. Soc.* **2002**, *124* (47), 14147−14155.

(12) Zhao, W.; Sun, J. Triflimide (HNTf$_2$) in Organic Synthesis. *Chem. Rev.* **2018**, *118* (20), 10349−10392.

(13) McCormack, A. C.; More O'Ferrall, R. A.; O'Donoghue, A. C.; Rao, S. N. Protonated Benzofuran, Anthracene, Naphthalene, Benzene, Ethene, and Ethyne: Measurements and Estimates of pKa and pK$_R$. *J. Am. Chem. Soc.* **2002**, *124* (29), 8575−8583.

(14) (a) Yuasa, J.; Yamada, S.; Fukuzumi, S. Detection of a radical cation of an NADH analogue in two-electron reduction of a protonated p-quinone derivative by an NADH analogue. *Angew. Chem., Int. Ed.* **2008**, *47* (6), 1068−1071. (b) Volkov, P. A.; Khrapova, K. O.; Telezhkin, A. A.; Ivanova, N. I.; Albanov, A. I.; Gusarova, N. K.; Trofimov, B. A. Catalyst-Free Phosphorylation of Acridine with Secondary Phosphine Chalcogenides: Nucleophilic Addition vs SN(H)Ar Reaction. *Org. Lett.* **2018**, *20*, 7388−7391.

(15) (a) Han, X.; Wu, J. Redox Chain Reaction—Indole and Pyrrole Alkylation with Unactivated Secondary Alcohols. *Angew. Chem.* **2013**, *125* (17), 4735−4738. (b) Xu, X. L.; Li, Z. Catalytic Electrophilic Alkylation of p-Quinones through a Redox Chain Reaction. *Angew. Chem., Int. Ed.* **2017**, *56* (28), 8196−8200. (c) Xu, X. L.; Li, Z. Deciphering the Redox Chain Mechanism in the Catalytic Alkylation of Quinones. *Synlett* **2018**, *29* (14), 1807−1813. (d) Xu, X. L.; Li, Z. Catalytic Redox Chain Ring Opening of Lactones with Quinones To Synthesize Quinone-Containing Carboxylic Acids. *Org. Lett.* **2019**, *21* (13), 5078−5081.

(16) (a) Handoo, K. L.; Gadru, K. Organic Reactive Intermediates: X. Preparation of Aromatic Cation Radicals by the Use of DDQ in Trifluoroacetic acid/ Dichloromethane Solvent System. *Curr. Sci.* **1986**, *55*, 920−922. (b) Eberson, L.; Hartshorn, M. P. On the existence of quinone radical cations. A study in 1,1,1,3,3,3-hexafluoropropan-2-ol. *J. Chem. Soc., Perkin Trans. 2* **1996**, No. 2, 151−154. (c) Nonella, M. Structures and Vibrational Spectra of p-Benzoquinone in Different Oxidation and Protonation States: A Density Functional Study. *J. Phys. Chem. B* **1997**, *101* (7), 1235−1246. (d) Zhai, L.; Shukla, R.; Rathore, R. Oxidative C−C Bond Formation (Scholl Reaction) with DDQ as an Efficient and Easily Recyclable Oxidant. *Org. Lett.* **2009**, *11* (15), 3474−3477.

(17) (a) Fukuzumi, S.; Ishikawa, M.; Tanaka, T. Acid-catalysed reduction of p-benzoquinone derivatives by an NADH analogue, 9,10-dihydro-10-methylacridine. The energetic comparison of one-electron vs. two-electron pathways. *J. Chem. Soc., Perkin Trans. 2* **1989**, No. 11,

1811−1816. (b) Fukuzumi, S.; Tokuda, Y. Outer-sphere electron-transfer oxidation of 10,10'-dimethyl-9,9',10,10'-tetrahydro-9,9'-biacridine. *J. Phys. Chem.* **1992**, *96* (21), 8409−8413. (c) Nguyen, T. L.; Lee, E. J.; Jeong, H.; Kim, B. K. Electrochemical Study of Ferrocene and Anthracene using Ultramicroelectrode in Chloroform over the Temperature Range of 25−50°C. *Bull. Korean Chem. Soc.* **2017**, *38* (7), 772−776.

(18) Li, G.; Zhou, S.; Su, G.; Liu, Y.; Wang, P. G. Improved synthesis of aryl-substituted anthracenes and heteroacenes. *J. Org. Chem.* **2007**, *72* (25), 9830−9833.

(19) Tsien, R. Y. The Green Fluorescent Protein. *Annu. Rev. Biochem.* **1998**, *67* (1), 509−544.

G